TRANSFORMATION OF THE STRUCTURE OF SILICON OXIDE DURING THE FORMATION OF Si NANOINCLUSIONS UNDER THERMAL ANNEALINGS

I.P. LISOVSKYY, M.V. VOITOVICH, A.V. SARIKOV, V.G. LITOVCHENKO, A.B. ROMANYUK[1], V.P. MELNYK, I.M. KHATSEVICH, P.E. SHEPELIAVYI

UDC 535.343.2

V. Lashkarev Institute of Semiconductor Physics, Nat. Acad. of Sci. of Ukraine
(41, Nauky Prosp., Kyiv 03028, Ukraine; e-mail: m@isp.kiev.ua),

[1]**Institute of Physics, University of Basel**
(82, Klingelbergstrasse, Basel 4056, Switzerland)

The composition and the structure of SiO_x films ($x = 1.16$, 1.3, and 1.6) as functions of the annealing temperature (600–1100 °C , 15 min, Ar atmosphere) are studied by infrared (IR) spectroscopy, photoluminescence (PL), and X-ray photoelectron spectroscopy (XPS). A correlation between the type of a structure (amorphous or crystalline) of Si nanoinclusions and the composition of the Si oxide matrix is found. Amorphous Si nanoinclusions are formed in the understoichiometric Si oxide matrix (SiO_x, $0 < x < 2$), while the formation of SiO_2 inclusions takes place under the Si nanocrystal formation. A physical model considering both a change of the chemical potential of amorphous Si with the temperature and the temperature-dependent crystallization of nanoinclusions is proposed to explain the observed correlation.

1. Introduction

At the present time, in order to produce Si nanoinclusions in the matrix of silicon oxide, the process of self-organization based on the thermally stimulated phase separation of nonstoichiometric films of SiO_x is widely used [1–3]. These films are preliminarily deposited on a substrate with the use of various methods (thermal deposition [1], implantation of Si ions into a layer of SiO_2 [2], chemical vacuum deposition (CVD) [3], *etc.*). In this case, the mode (temperature, duration) of a thermal treatment of SiO_x films (temperature and duration of the annealing) plays a crucial role, by determining the degree of decomposition of silicon oxide and, respectively, the amount of formed Si nanoinclusions, the composition and structure of the oxide matrix, and the nanoinclusion–matrix boundary. It is known that Si nanoinclusions are amorphous at relatively low temperatures of the annealing (∼700 °C), whereas Si nanocrystals are formed at high temperatures (∼1100 °C) [4,5]. On the other hand, an increase of the temperature of a thermal treatment leads to a growth of the degree of stoichiometry of the oxide matrix after annealings: if the matrix is nonstoichiometric Si oxide with the stoichiometry index $x < 2$ as a result of the annealing at a temperature of 700 °C, then it is completely transformed into stoichiometric silicon dioxide after annealings at 1100 °C [6]. This dependence of structural characteristics of the system on the temperature can have a quite nontrivial physical nature, i.e., we can speak about a possible interrelation between the structure of Si nanoinclusions and the composition of the surrounding oxide matrix. In order to reveal such an interrelation, we subjected films of SiO_x to thermal treatments in a wide temperature range. In this case, we controlled both the structure and composition of the matrix, as well as the structural state of Si nanoinclusions.

2. Experimental Procedure

Films of SiO_x with the initial compositions x equal to 1.16, 1.30, and 1.60 were produced by vacuum spraying of a SiO powder (purity of 99.9%, the production of "Cerac Inc.") onto two-sided polished Si plates heated up to 150 °C at a residual pressure in the vacuum chamber of $\sim 10^{-4}$–10^{-5} Pa. Thicknesses of the obtained films were determined with a profilometer Dektak 3030 and were equal to ≈340 nm. Thermal annealings of films were performed at temperatures from 600 to 1100 °C for 5–100 min in the atmosphere of pure Ar.

The IR-transmission spectra of the structures of Si-SiO_x were measured with the use of a Fourier spectrometer Spectrum BXII PerkinElmer with a resolving power of 4 cm^{-1}, and the transmission spectra of a Si substrate were used for comparison. The composition of the films of SiO_x was determined from the dependence of a position of the maximum of the basic absorption band (ν_M) on x in the interval

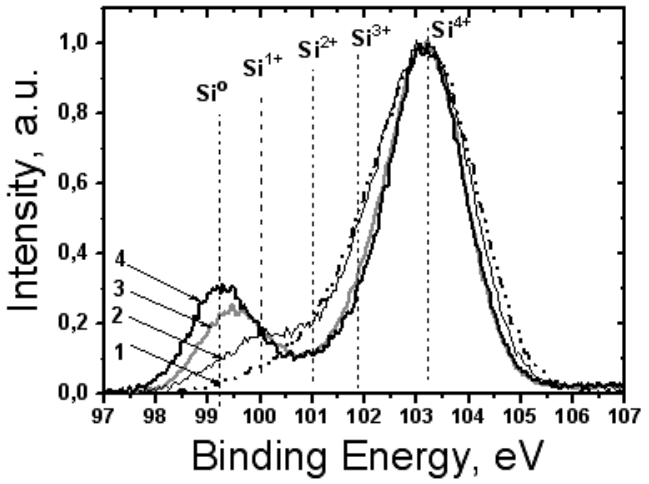

Fig. 1. XPS Si-2p spectra of SiO_x films: initial (*1*) and annealed in Ar atmosphere during 15 min at 700 (*2*), 900 (*3*), and 1100 °C (*4*)

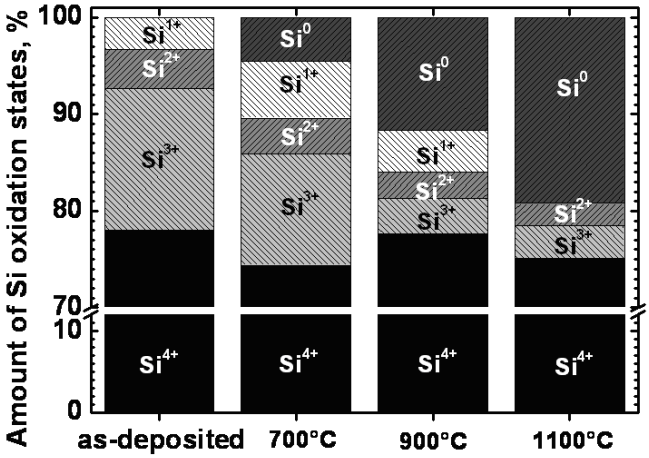

Fig. 2. Contributions of oxidized Si states in SiO_x films ($x = 1.6$) prior to annealing and annealed at different temperatures

$1000 \leq \nu_M \leq 1100$ cm^{-1} [7]. The basic absorption band was decomposed into elementary components of the Gauss form which correspond to the absorption by bonds Si–O belonging to the compositions of various molecular complexes SiO_ySi_{4-y} ($1 \leq y \leq 4$). A share of the latter in the film structure was evaluated by the earlier proposed method [8] in the frame of the model of random bonds [9].

The X-ray photoelectron spectra were registered with the help of a VG ESCALAB 210 system equipped with a monochromatic emission source Al K_α (1486.6 eV) with a resolution of 0.32 eV. The energy calibration was realized by the binding energy of level $4f_{7/2}$ of specimens made of pure Au at 84.0 eV.

The photoluminescence spectra were measured at room temperature in the wavelength interval from 550 to 1000 nm under the excitation by the beam of a semiconductor laser with a wavelength of 473 nm. The emission power was about 50 mW. The obtained PL spectra were corrected with regard for the spectral sensitivity of the measuring setup. We analyzed the form of PL spectra, by using their mathematical decomposition into components of the Gauss form.

3. Experimental Results and Their Discussion

3.1. X-ray photoelectron spectroscopy

In Fig. 1, we present the Si-2p spectra of SiO_x films annealed at temperatures of 700, 900, and 1100 °C. The decomposition of the obtained curves into Gauss profiles according to the procedure given in work [10] allowed us to separate five types of molecular complexes which are characterized by different chemical environment of the central Si atom. The first Gauss component Si^0 with the maximum at 99.2 eV corresponds to the emission of photoelectrons from clusters of elementary Si ($SiSi_4$). The components related to Si in different states of oxidation (Si^{n+}) are shifted relative to the Si^0 line by 0.95, 1.85, 2.55, and 3.95 eV and have half-widths of 1.05, 1.15, 1.23, and 1.61 eV for complexes with n= 1–4 (i.e., complexes $SiOSi_3$, SiO_2Si_2, SiO_3Si, and SiO_4), respectively, which agrees quite well with the results of work [11]. The relative contents of the components versus the annealing temperature are shown in Fig. 2. It is seen that the relative concentration of elementary Si increases monotonously in the temperature interval 700 – 1100 °C. The concentration of molecular clusters of underoxidized Si decreases, so that their concentration becomes rather small as a result of annealings at a temperature of 1100 °C.

3.2. IR-spectroscopy

The IR absorption spectra of several specimens under study are presented in Fig. 3. It is seen that, as a result of annealings of the initial film of nonstoichiometric silicon oxide, the band maximum for the absorption on Si–O bonds is shifted to the side of larger wave numbers, and the area of this band increases (Fig. 3,*b*, *c*, *d*). An increase of the annealing temperature enhances both effects. These facts indicate that the thermal treatment of SiO_x films induces an increase of both the stoichiometry index of the oxide matrix, x, and the relative concentration of interstitial oxygen (bonds Si–O–Si). The mentioned facts well agree with the known literature data [4, 12].

Let us consider the process of transformation of a structural state of oxygen in a SiO_x film as a function of the annealing temperature in more details.

The absorption band of films annealed at 700 °C has a maximum in the region of 1040–1064 cm^{-1} (depending on the stoichiometry index of the initial specimen), which corresponds to $1.45 \leq x \leq 1.75$ and, like the IR spectrum of the initial film (Fig. 3,*a*), is described with the sufficient accuracy by the sum of elementary components inherent to the SiO_x phase [9, 13] (Fig. 3,*b*). The data obtained by X-ray photoelectron spectroscopy show a rather large concentration of underoxidized Si in such specimens, though it is lower than that in an as-sprayed film. Earlier, it was demonstrated that a similar film is not dissolved practically in a 5%-solution of HF [14]. The above-presented facts allow us to conclude that the matrix of silicon oxide remains nonstoichiometric after annealings at 700 °C, and its structure can be represented in the form of a mixture of molecular complexes SiO_ySiO_{4-y} with $1 \leq y \leq 4$ [9, 13].

The absorption band of SiO_x films annealed at 1100 °C has maximum at 1095 cm^{-1} irrespective of the stoichiometry index of the initial specimen. It corresponds to $x \approx 2$ and is described with the sufficient accuracy by the sum of elementary components inherent to the SiO_2 phase (Fig. 3,*d*). The amount of underoxidized Si (Fig. 2) in such a film is very smal. We may conclude that, after the annealing at 1100 °C, the matrix of silicon oxide became stoichiometric with the composition of SiO_2, and its structure can be mainly represented as the lattice of interdependent 4- and 6-membered rings of SiO_4 tetrahedra [15]. Some amount of molecular clusters SiO_2Si_2 and SiO_3Si which are registered by X-ray photoelectron spectroscopy belongs, most probably, to the transient layer on the Si nanoinclusions–SiO_2 matrix boundary.

In the case of specimens annealed at intermediate temperatures (800 – 1000 °C), the situation concerning the matrix structure is more complicated. For SiO_x films with the highest initial index of stoichiometry (x=1.6) which were annealed at temperatures of 800–900 °C, the position of the maximum of the IR-absorption band (1076 cm^{-1}) corresponds to the SiO_x phase with x = 1.92. However, after the thermal treatment at 1000 °C, the absorption band of films even with the lowest value of the stoichiometry index (x = 1.16) is shifted to ν_M =1080 cm^{-1}, which is characteristic of the SiO_2 phase. At the same time, the absorption band for such films cannot be represented by a superposition of only two main Gauss profiles inherent to the SiO_2 phase ($\approx$ 1055 and $\approx$ 1090 cm^{-1}) [15], but it is well described by a collection of profiles characteristic of the SiO_x phase. On the other hand, the data of X-ray photoelectron spectroscopy (Fig. 2) demonstrate the presence of molecular complexes of underoxidized Si in a remarkable concentration in such films, though their share is sufficiently small as compared with the concentration of SiO_4 tetrahedra. Films of SiO_x annealed at 1000 °C were sufficiently well dissolved in a 5%-solution of HF. However, the rate of their dissolution was thrice less than that of a layer of SiO_2 [14].

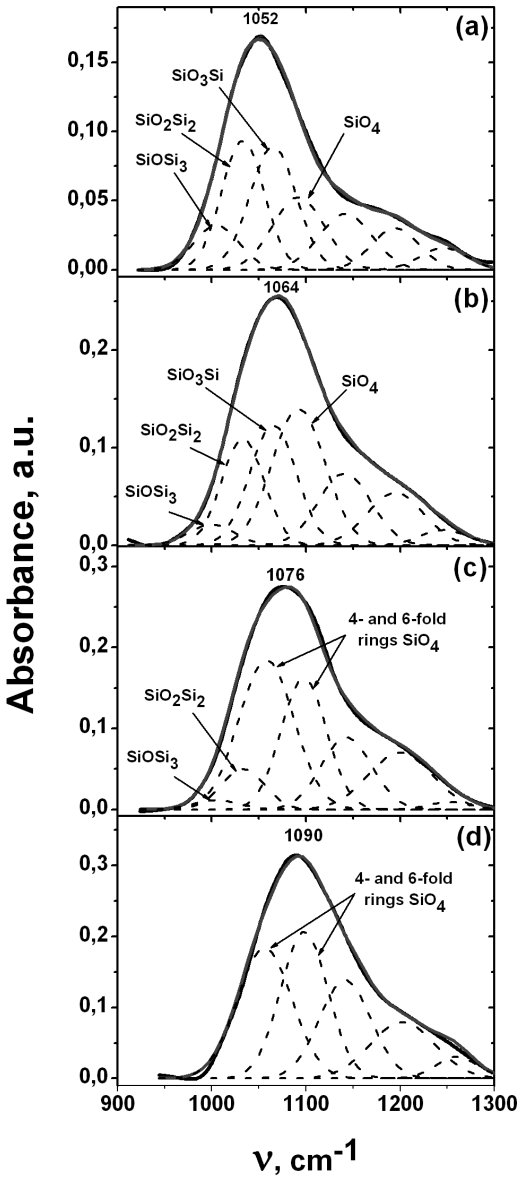

Fig. 3. IR-spectra of SiO_x films: initial (*1*) and annealed at 700 (*2*), 900 (*3*), and 1100 °C (*4*)

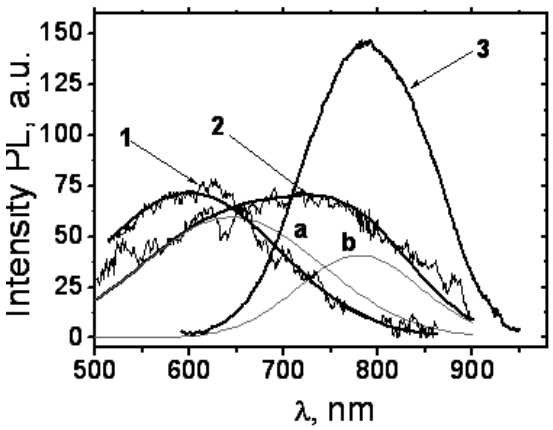

Fig. 4. *1* – 700 °C, *2* – 900 °C, *3* – 1100 °C (15 min, Ar) reduced by 6 times

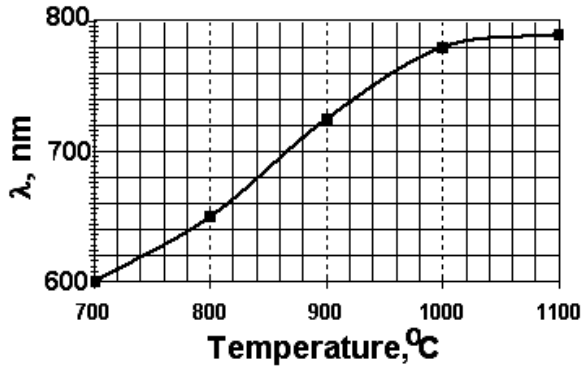

Fig. 5. Dependence of PL maximum position on annealing temperature (700–1100 °C)

In view of the above-presented discussion, it would be possible to assume that the matrix of specimens annealed at temperatures 800–1000 °C is, on the whole, nonstoichiometric Si oxide. That is, this matrix is composed by randomly distributed interdependent complexes SiO_ySi_{4-y} ($1 \leq y \leq 4$), and the content of SiO_4 tetrahedra ($y = 4$) exceeds considerably the content of clusters of the other types. However in this case, we must observe a significantly better coupling of SiO_4 tetrahedra with one another, i.e., local inclusions of the SiO_2 phase should be formed. This hypothesis is corroborated by experimental results. For example, according to the data of X-ray photoelectron spectroscopy, a share of clusters of underoxidized Si decreases monotonously with increase of the annealing temperature (Fig. 2). In order to observe the same monotonous decrease of the areas of corresponding components of the IR-absorption bands, it is necessary to add a band with the maximum at $\approx$1055 cm^{-1} (SiO_4 tetrahedra bound into 4-membered rings) to the decomposition which contains also the Gauss component at $\sim$1070 cm^{-1} (complexes SiO_3Si) (Fig. 3, *c*). Thus, the matrix of specimens annealed at temperatures 800–1000 °C is, most probably, inhomogeneous and is composed from a mixture of the SiO_x and SiO_2 phases, and the bulk share of the SiO_2 phase increases with the annealing temperature.

3.3. Photoluminescence

The initial films of silicon oxide did not demonstrate photoluminescence which appeared only after the annealing of specimens. The maximum position of the PL band (Fig. 5), its shape, and the emission intensity depended significantly on the annealing temperature (at the same duration of thermal treatments).

In Fig. 4, we give the PL spectra of specimens under study and the elementary components (for a complex spectral band). We can conclude the following: 1) at a low annealing temperature (700 °C), the PL band is simple and is described by a single Gauss profile with the maximum at 650 ±50 nm and a half-width of 220 nm (Fig. 4, curve *1*); (2) at the high annealing temperature (1100 °C), the PL band is also simple and is described by a Gauss profile with the maximum at 790 ± 10 nm and a half-width of 155 nm (Fig. 4, curve *3*); (3) at intermediate temperatures (800–1000 °C), the PL band is complicated (Fig. 4, curve *2*) and is described, with high accuracy, by a sum of two above-mentioned profiles (Fig. 4,*a*,*b*), moreover, the component with the maximum at 790 nm is very weak for a specimen annealed at 800 °C; (4) the above-mentioned dependence of the position of the PL band maximum on the thermal treatment temperature is related to a change of the contribution of elementary profiles with variation of the temperature. This fact is illustrated in Fig. 5.

The annealing duration did not practically affect the intensity of the elementary PL band with the maximum at 650±50 nm irrespective to the temperature. At the same time, the PL band intensity with the maximum at 790 nm depended significantly on the duration of a thermal treatment (Fig. 6); in particular, its increase by almost a factor of 3 was observed as a result of thermal treatments at 1100 °C during 100 min of the annealing, as compared with the PL intensity during the annealing for 5 min.

It is known [4, 5] that the thermally stimulated phase decomposition of SiO_x is accompanied by the formation of nanoinclusions of amorphous Si (naSi)

at low annealing temperatures (700–800 °C), which emit light with a maximum in the region of 600–750 nm [4, 16], and nanocrystals of Si (ncSi) under high-temperature (more than 1000 °C) treatments, whose PL band lies in the region of wavelengths from 780–850 nm [1, 5]. Similar results were also obtained on the specimens studied in the present work with the use of Raman light scattering [17], ellipsometry [18], and high-resolution transmission electron microscopy [19]. In particular, it was shown that, under high-temperature annealings of SiO_x films, Si nanocrystalline inclusions with an average size of 3 nm are formed. According to the experimental data [20] and the theoretical calculations [21], Si nanoparticles of such sizes emit light with a maximum in the region of 780–850 nm, which agrees well with our experimental results. Therefore, we conclude that the elementary PL band with the maximum at 650±50 nm and a half-width of 220 nm is related just to inclusions of naSi, whereas the elementary PL band with the maximum at 790 nm and a half-width of 155 nm corresponds to ncSi.

4. Theoretical Model

In this section, we propose a theoretical model for the description of the experimentally observed correlation between the presence of amorphous Si inclusions and nonstoichiometric Si oxide, on the one hand, and, on the other hand, the correlation between the formation of Si nanocrystals and the creation of stoichiometric SiO_2 in the matrix of silicon oxide in the frame of the phase decay model based on the equality of the chemical potentials of Si in precipitates and the oxide phase.

As known, during a high-temperature annealing of SiO_x films, there occurs the separation of phases accompanied by the precipitation of Si by the reaction [22]

$$y\mathrm{SiO}_x \rightarrow (y-x)\mathrm{Si} + x\mathrm{SiO}_y (x < y \leq 2), \quad (1)$$

where x and y are the coefficients of stoichiometry of a film before and after the annealing, respectively.

In this case, silicon can precipitate into the crystalline or amorphous phase depending on the annealing temperature, as was shown experimentally [16–22]. The final state of a film involves the equilibrium between Si precipitates and the environment of silicon oxide. Accoding to the classical positions of thermodynamics [23], the equilibrium state of two phases in the case of the exchange by a substance is realized under the equality of the chemical potentials of a transferred substance in both phases. In the case of the phase separation under the annealing of nonstoichiometric films of SiO_x, this means the equality of the chemical potentials of Si in precipitates and the oxide matrix:

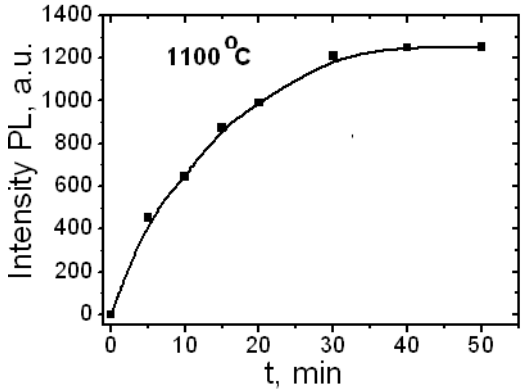

Fig. 6. Dependence of PL band at 890 nm on time of annealing at 1100 °C

$$\mu_{\mathrm{Si}}^{pre} = \mu_{\mathrm{Si}}^{\mathrm{SiO}_x}, \quad (2)$$

Here, the right- and left-hand sides are the chemical potentials of Si in the phase of precipitated Si and in the phase of silicon oxide, respectively. This equality is the base for the construction of a model of phase separation under the annealing of nonstoichiometric films of SiO_x.

Values of the chemical potential of amorphous Si can be determined relative to that of crystalline Si [24]. The corresponding temperature dependence an be approximated by a linear function in the form [25]

$$\mu_{\mathrm{Si}}^{a-\mathrm{Si}} = \mu_{\mathrm{Si}}^{c-\mathrm{Si}} + \frac{h_E - s_E T}{N_{\mathrm{A}}}, \quad (3)$$

where $\mu_{\mathrm{Si}}^{a-\mathrm{Si}}$ and $\mu_{\mathrm{Si}}^{c-\mathrm{Si}}$ are, respectively, the chemical potentials of Si in the amorphous and crystalline phases, h_E is the molar enthalpy of the crystallization, s_E is the molar excess entropy, T is the absolute temperature, and $N_A = 6.022{\times}10^{23}$ mole^{-1} is the Avogadro constant.

According to the formula for ideal solutions, the chemical potential of Si in the matrix of silicon oxide can be presented in the form [23]

$$\mu_{\mathrm{Si}} = \mu_{\mathrm{Si}}^0 + kT \ln C_{\mathrm{Si}}, \quad (4)$$

where μ_{Si}^0 is the standard value of the chemical potential [25], $k = 1.38{\times}10^{-23}$ J/K is the Boltzmann constant, and C_{Si} is the concentration of Si in the matrix of silicon oxide. Since the atomic concentration in the phase of silicon oxide is slightly varied with the composition (at

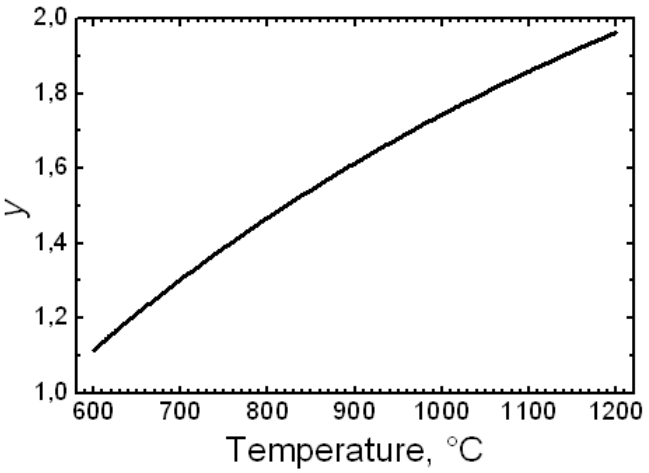

Fig. 7. Calculated dependence of the equilibrium stoichiometry index x of SiO_x films annealed at different temperatures

most 20%), we can take it, for simplicity, invariable and equal to the atomic concentration in the SiO_2 phase, $C_0 \approx 7\times10^{22}$ cm^{-3} [26]. In this case for the given x, the concentration of Si in the SiO_x phase is as follows:

$$C_{\rm Si}^{{\rm SiO}_x} = \frac{C_0}{1+x}. \tag{5}$$

Here, the upper symbol indicates that we deal with the nonstoichiometric phase of SiO_x.

The analogous formula for the concentration of Si in stoichiometric SiO_2 takes the form

$$C_{\rm Si}^{{\rm SiO}_2} = \frac{C_0}{3}. \tag{6}$$

In order to determine the chemical potential of crystalline Si, we use the formula analogous to formula (2), by taking into account that the SiO_2 phase is in equilibrium with crystalline Si. We are based on the facts that the oxidation of crystalline Si is accompanied by the formation of stoichiometric SiO_2 on its surface, and the boundary between Si and silicon oxide is sharp under the carefully performed process of oxidation, i.e., the transient layer does not exceed one-two monolayers. The absence of the migration of Si and oxide and the formation of a transient region with the composition which is smoothly varied correspond to the state of equilibrium between Si and stoichiometric silicon oxide and, respectively, to the equality of the chemical potentials of Si in both phases:

$$\mu_{\rm Si}^{\rm c-Si} = \mu_{\rm Si}^{\rm SiO_2}. \tag{7}$$

Comparing formulas (2)–(7), we can obtain the following formula for the stoichiometry index of silicon oxide under the phase separation of nonstoichiometric films of SiO_x under a high-temperature annealing [see formula (1)]:

$$y = 3\exp\left(-\frac{h_E - s_E T}{N_{\rm A} kT}\right) - 1. \tag{8}$$

In Fig. 7, we present the dependence of y on the temperature which is determined according to formula (8). The value $S_E = 3.97$ J/mole·K corresponds to a relaxed structure of amorphous silicon in agreement with the experimental data given in [24]. The literature gives various values for h_E in the region $\approx$ 9.5–25 kJ/mole [27]. We used this parameter as the fitting one and obtained $h_E = 6$ kJ/mole. The last value coincides with the literature data by the order of magnitude. It is worth noting that the above-presented values of molar enthalpy of the crystallization are related to bulk amorphous Si. The difference of the numerical values of h obtained by us and given by the literature can be related to the difference of the structures of amorphous Si which is formed in the bulk and Si precipitates under the phase decomposition of nonstoichiometric films of SiO_x.

Up to now, we considered the equilibrium between inclusions of amorphous Si and the oxide matrix, at which the complete phase separation for $y = 2$ cannot occur at all temperatures lower than the melting temperature of amorphous Si [24, 27]. At the same time, the experimentally revealed presence of stoichiometric SiO_2 and crystalline Si inclusions, as well as their correlation, can be explained in the following manner.

Work [28] proposed a model which describes a shift of the crystallization temperature of planar layers of amorphous Si positioned between layers of silicon oxide. Assuming that a similar model can be also applied to the case of nano-sized Si inclusions in the oxide matrix, we may conclude that the crystallization of inclusions is possible in the case where their size is more than a certain value which depends on the temperature as follows: $R_{\rm cr} \sim \ln[(T_{\rm m} - T_{\rm ac})/(T - T_{\rm ac})]$. Here, $T_{\rm ac}$ and $T_{\rm m}$ are the crystallization temperatures of bulk amorphous Si and crystalline Si, respectively, and $R_{\rm cr}$ is the critical radius of a Si inclusion. This fact and the increase of the average size of inclusions with the annealing temperature [29] are responsible for the temperature shift of a share of crystalline Si in annealed films of SiO_x.

Under the crystallization of amorphous Si, the chemical potential of Si atoms decreases and becomes

equal to the chemical potential of Si in the SiO_2 phase. This promotes the additional redistribution of atoms of oxygen and silicon near Si inlcusions with the formation of a local structure of SiO_2. A similar idea of the formation of shells from the SiO_2 phase near Si inclusions was advanced earlier in work [30], where the authors indicated that such a situation happens always under the phase separation in the course of annealing of nonstoichiometric films of SiO_x. In the present work, we have shown that such shells with the stoichiometric composition should be formed only near crystalline inclusions of Si. This fact is responsible for the experimentally observed correlation between the presence of crystalline inclusions of Si and the SiO_2 phase in SiO_x films annealed at high temperatures.

5. Conclusions

In the present work, we have studied the processes of phase separation in nonstoichiometric films of SiO_x under high-temperature annealings leading to the formation of the phases of amorphous Si and crystalline Si which differ in their structures, as well as to an increase of the stoichiometry index of the matrix of silicon oxide and the formation of the SiO_2 phase. We have established the correlation between the formation of crystalline Si nanoinclusions and the formation of stoichiometric silicon oxide, as well as that between the formation of amorphous Si inclusions and the presence of nonstoichiometric silicon oxide in such films. To explain the structural peculiarities of SiO_x films with built-in Si nanoinclusions formed at various annealing temperatures, we proposed a physical model which considers the thermodynamical equilibrium between the matrix of silicon oxide and the phase of precipitated Si. The stoichiometry index of the oxide matrix after annealings is determined by the equality of the chemical potentials of silicon in both phases. The increase of the stoichiometry index in the course of the formation of Si nanocrystals is explained by a decrease of the chemical potential of crystalline Si as compared with that of amorphous Si and, thus, by a shift of the equilibrium to the side of the precipitation of Si from the oxide matrix.

1. D. Nesheva, I. Bineva, Z. Levi, Z. Aneva, Ts. Merdzhanova, and J.C. Pivin, Vacuum **68**, 1 (2002).
2. B. Garrido, M. Lopez, C. Garcia, A. Perez-Rodriguez, J.R. Morante, C. Bonafos, M. Carrada, and A. Claverie, J. Appl. Phys. **91**, 798 (2002).
3. F. Priolo, G. Franzt, D. Pacifici, V. Vinguerra, F. Iacona, and A. Irrera, J. Appl. Phys. **89**, 264 (2001).
4. H. Rinnert, M. Vergnat, and A. Burneau, J. Appl. Phys. **89**, 237 (2001).
5. Y. Kanzawa, T. Kageyama, S. Takeoka, M. Fujii, S. Hayashi, and K. Yamamoto, Solid State Commun. **102**, 533 (1997).
6. V.A. Dan'ko, I.Z. Indutnyi, V.S. Lysenko, I.Yu. Maidanchuk, V.I. Min'ko, A.N. Nazarov, A.S. Tkachenko, and P.E. Shepelyavyi, Semiconductors **39**, 1197 (2005).
7. M. Nakamura, V. Mochizuki, K. Usami, U. Yoto, and T. Nozaki, Solid State Commun. **50**, 1079 (1984).
8. I.P. Lisovskii, V.G. Litovchenko, V.B. Lozinskii, S.I. Frolov, H. Flietner, W. Füssel, and E.G. Schmidt, J. Non-Cryst. Solids **187**, 91 (1995).
9. H.R. Philipp, J. Phys. Chem. Solids **32**, 1935 (1971).
10. D.A. Shirley, Phys. Rev. B. **5**, 4709 (1972).
11. S. Kim, M.C. Kim, S.-H. Choi, K.J. Kim, H.N. Hwang, and C.C. Hwang, Appl. Phys. Lett. **91**, 103113 (2007).
12. T.P. Chen, Y. Liu, C.Q. Sun, M.S. Tse, J.H. Hsieh, Y.Q. Fu, Y.C. Eiu, and S. Fung, J. Phys. Chem. B **108**, 16609 (2004).
13. G. Pérez and J.M. Samz, Thin Solid Films **416**, 24 (2002).
14. I.Z. Indutnyy, I.P. Lisovskyy, D.O. Mazunov, P.E. Shepeliavyi, G.Yu. Rudko, and V.A. Dan'ko, Semiconductor Physics, Quantum Electronics & Optoelectronics **7**, 161 (2004).
15. I.P. Lisovskii, V.G. Litovchenko, V.B. Lozinskii, and G.I. Steblovskii, Thin Solid Films **213**, 164 (1992).
16. D. Nesheva, C. Raptis, A. Perakis, I. Bineva, Z. Aneva, Z. Levi, S. Alexandrova, and H. Hofmeister, J. Appl. Phys. **92**, 4678 (2002).
17. V.Ya. Bratus', V.A. Yukhimchuk, L.I. Berezhinsky, M.Ya. Valakh, I.P. Vorona, I.Z. Indutnyi, T.T. Petrenko, P.E. Shepeliavyi, and I.B. Yanchuk, Semiconductors **35**, 821 (2001).
18. I.P. Lisovskyy, I.Z. Indutnyy, B.N. Gnennyi, P.M. Litvin, D.O. Mazunov, A.S. Oberemok, N.V. Sopinskii, and P.E. Shepelyavyi, Fiz. Tekhn. Polupr. **37**, 98 (2003).
19. A. Szekeres, T. Nikolova, A. Paneva, A. Cziraki, Gy.J. Kovacs, I. Lisovskyy, D. Mazunov, I. Indutnyy, and P. Shepeliavyi, Mater. Sci. Engin. B, **124-125**, 504 (2005).
20. U. Kahler and H. Hofmeister,Appl. Phys. A **74**, 13 (2002).
21. N.A. Hill and K.B. Whaley, Phys. Rev. Lett. **75**, 1130 (1995)
22. M. Zacharias, J. Heitmann, R. Scholz, U. Kahler, M. Schmidt, and J. Bläsing, Appl. Phys. Lett. **80**, 661 (2002).
23. R. Kubo, *Thermodynamics* (North-Holland, Amsterdam, 1968).
24. C. Spinella, S. Lombardo, and F. Priolo, J. Appl. Phys. **84**, 5383 (1998).

25. O. Nast, The Aluminum-Induced Layer Exchange Forming Polycrystalline Silicon on Glass for Thin-Film Solar Cells, Dissertation, Philipps-Universität Marburg, 2000.

26. A. La Magna, G. Nicotra, C. Bongiorno, C. Spinella, M.G. Grimaldi, E. Rimini, L. Caristia, and S. Coffa, Appl. Phys. Lett. **90**, 183101 (2007).

27. P.A. Stolk, F.W. Saris, A.J.M. Berntsen, W.F. van der Weg, L.T. Sealy, R.C. Barklie, G. Krötz, and G. Müller, J. Appl. Phys. **75**, 7266 (1994).

28. M. Zacharias and P. Streitenberger, Phys. Rev. B **62**, 8391 (2000).

29. D. Comedi, O.H.Y. Zalloum, E.A. Irving, J. Wojcik, T. Roschuk, M.J. Flynn, and P. Mascher, J. Appl. Phys. **99**, 023518 (2006).

30. B.J. Hinds, F. Wang, D.M. Wolfe, C.L. Hinkle, and G. Lucovsky, J. Vac. Sci. Technol. B **16**, 2171 (1998).

Received 11.03.09.
Translated from Ukrainian by V.V. Kukhtin

ТРАНСФОРМАЦІЯ СТРУКТУРИ ОКСИДУ КРЕМНІЮ В ПРОЦЕСІ ФОРМУВАННЯ КРЕМНІЄВИХ НАНОВКЛЮЧЕНЬ ПРИ ТЕРМІЧНИХ ВІДПАЛАХ

І.П. Лісовський, М.В. Войтович, А.В. Саріков, В.Г. Литовченко, А.Б. Романюк, В.П. Мельник, І.М. Хацевич, П.Є Шепелявий

Р е з ю м е

Методами інфрачервоної (ІЧ) спектроскопії, фотолюмінесценції (ФЛ) та рентгенівської фотоелектронної спектроскопії (XPS) досліджено склад та структуру плівок SiO_x (x =1,16, 1,3, 1,6) залежно від температури відпалу (600–1100 °C, 15 хв, атмосфера Ar). Встановлено кореляцію між типом структури (аморфна, кристалічна) нановключень кремнію і складом оксидної матриці: аморфні нановключення кремнію утворюються в матриці оксиду кремнію з нестехіометричним складом (SiO_x, $0< x <2$), тоді як за наявності кремнієвих нанокристалів спостерігається формування ділянок стехіометричної фази оксиду кремнію ($x = 2$). Для пояснення спостереженої кореляції запропоновано фізичну модель, що враховує зміну з температурою хімічного потенціалу аморфного кремнію та температурно-залежну кристалізацію нановключень.